

1 Aerosol emission is increased in 2 professional singing

3 **Dirk Mürbe^{1†}, Martin Kriegel^{2†}, Julia Lange², Hansjörg Rotheudt², Mario Fleischer¹**

*For correspondence:

4 dirk.muerbe@charite.de (Dirk Mürbe); m.kriegel@tu-berlin.de (Martin Kriegel)

5 ¹Charité – Universitätsmedizin Berlin, Department of Audiology and Phoniatics, Berlin, Germany; ²Technische Universität Berlin, Hermann-Rietschel-Institut, Berlin, Germany

6 [†]These authors contributed equally to this work

7 **Abstract** In this study, emission rates of aerosols emitted by professional singers were
8 measured with a laser particle counter under cleanroom conditions. The particle source strengths
9 during singing varied between 753.4 and 6095.37 P/s. Particle source strengths for singing were
10 compared with published data for breathing and speaking. Significantly higher emission rates were
11 found for singing. The growth rates between singing and speaking were between 3.97 and 99.54.
12 Further, effects of vocal loudness and gender were investigated. The present study should support
13 the efforts to improve the risk management in cases of possible aerogenic virus transmission,
14 especially for choir singing.

16 Introduction

17 The respiratory system is the main transmission route for SARS-CoV-2-viruses. (*Asadi et al., 2020a*;
18 *Morawska and Cao, 2020*).

19 Depending on particle size, a distinction can be made between droplets with a diameter greater
20 than 5 µm and particles smaller than 5 µm (aerosols or droplet nuclei) (*Couch et al., 1966*; *Tellier,*
21 *2006*; *Judson and Munster, 2019*). Droplets and aerosols differ according to the influence of gravity.
22 For example, droplets of a size of 100 µm sink to the ground within a short time and are transported
23 up to a distance of 1.5 m (*Kähler and Hain, 2020*; *Wei and Li, 2015*).

24 When aerosols are exhaled, the fluid component of the pathogen-containing particles evaporates
25 more and more. They become lighter, can float in the air for longer periods and spread in closed

26 rooms by air flow and diffusion (*Stadnytskyi et al., 2020*). As the basis of a possible aerogenic
27 transmission of the SARS-CoV-2-virus, the spatial distribution of aerosols is dependent on several
28 factors of the surrounding air, such as temperature and humidity (*Morawska, 2006*).

29 Droplets and aerosols are also produced during speaking and singing, because the respiratory
30 tract has a dual function: it is not only the main tool for ventilation, but also the source of voice and
31 spoken language production. Particle formation in the pulmonary alveoli (*Johnson and Morawska,*
32 *2009*), flow effects of the vibrating vocal folds and adjustments of the articulation instruments are
33 regarded as aerosol generating mechanisms (*Johnson et al., 2011*).

34 In comparison to breathing, a stronger formation of aerosols is known for speaking, whereby
35 also a dependence of the number of the arising particles on vocal loudness is described (*Hartmann*
36 *et al., 2020; Asadi et al., 2020b*). For singing, a significantly higher aerosol production is assumed,
37 probably due to the underlying physiological mechanisms and the greater continuity of voice
38 production over time. This assumption is supported by reports of high infection rates during choir
39 rehearsals in closed rooms (*Hamner et al., 2020*).

40 Previous measurements focus on fluid mechanical aspects in the near-field plume of the mouth
41 during singing (*Anfinrud et al., 2020; Kähler and Hain, 2020*). The spread of the emitted droplets is
42 investigated, hence distance rules can be derived for protection against droplet infection. However,
43 a risk assessment including the distribution of aerosols in larger rooms is not possible with this
44 method.

45 The current investigations aim to initially determine the number and size distribution of even
46 small particles emitted by professional singers during singing. This information can be the basis for
47 a numerical calculation of the distribution of aerosols in larger rooms, which takes into account the
48 boundary conditions being typical for concert and opera performances.

49 The present data may contribute to improved risk management strategies in the fields of culture
50 and education. They should be used for specification of hygiene measures and ventilation concepts
51 in order to facilitate performances and events.

52 Results

53

54 Particle size distribution

55 The particle count measurement method detects different sizes of particles from 0.3 μm to 25 μm .
 56 As shown in the log-probability plot (**Figure 1**), > 99 % of all detected particles were $\leq 5 \mu\text{m}$ (> 80 % of
 57 all particles $\leq 1 \mu\text{m}$). Based on this observation, and following the agreement that aerosol particles
 58 of size $\leq 5 \mu\text{m}$ are referred to as aerosol particles, the following results are given for particles of
 59 size 0.3 μm – 5 μm .

60

61 **Experiment I**

62 **Figure 2** illustrates both the particle source strengths (emission rates) for the different test
 63 conditions (breathing, speaking, and singing) and the maximum sound pressure levels for singing.

64 The results confirm the hypothesis of higher emission rates for singing compared to breathing
 65 and speaking.

66 While the individual median values for singing ranged from 753.36 P/s (S5) to 6095.37 P/s (S2)
 67 (**Appendix 1, Table 1**), those for speaking ranged from 14.13 P/s (S6) to 390.84 P/s (S2) (**Appendix 1,**
 68 **Table 2**). The individual median values for breathing ranged from 4.71 P/s (S1) to 428.55 (S2)
 69 (**Appendix 1, Table 3**).

70 The growth rate of the emission rates for singing in comparison to speaking was between 3.97
 71 (S1) and 99.54 (S2). Moreover, the growth rate of the emission rates for singing in comparison to
 72 breathing was between 14.22 (S2) and 329.61 (S1) (**Table 1**).

73 The evaluation of the sound pressure levels showed that the higher voice classifications soprano
 74 (female) and tenor (male) had the expected higher sound pressure levels than the lower voice
 75 classifications alto and baritone. While the maximum sound pressure level of males in the selected
 76 sample were always positively correlated with the particle emission rate, there was no clear
 77 correlation in this respect for the female voices.

78 Statistical analysis by means of linear mixed modeling (**Eq. 2**) showed significant differences
 79 of the (logarithmic) particle source strength $\log_{10} P_M$ between the different test conditions breath-
 80 ing, speaking and singing. Condition affected $\log_{10} P_M$ ($\chi^2(2)=37.797$, $p=6.2 \cdot 10^{-9}$) increasing it
 81 by a factor of 0.5230 ± 0.2664 (standard errors) from breathing to speaking and by a factor of
 82 1.7740 ± 0.1211 (standard errors) from breathing to singing. By-subject analysis turned out that S2
 83 and S6 showed a decrease of emitted particles from breathing to speaking (see **Figure 2**). Further,
 84 female singers showed significantly higher particle source strengths than males. Gender affected

85 $\log_{10} P_M$ ($\chi^2(1)=4.3035$, $p=0.03803$) lowering it by a factor of -0.3453 ± 0.1246 (standard errors) from
 86 female to male.

87

88 Experiment II

89 The results of measurements with the sustained vowel /a/ at different loudness conditions are
 90 presented in **Figure 3**. Seven of the eight subjects showed an increase in the emission rate with
 91 increasing loudness. The comparison of piano (**Appendix 1, Table 4**) and forte (**Appendix 1, Table 5**)
 92 showed a growth rate up to 114.29 (S3) (**Table 1**). There were higher emission rates for singing in
 93 forte for females (from 2023.02 P/s (S1) to 8072.35 P/s (S3)) compared to males (from 376.7 P/s
 94 (S5) to 2851.02 P/s (S7)). The same implications were made during the increase from piano to
 95 mezzo-forte (see also **Appendix 1, Table 6**).

96 Statistical analysis by means of linear mixed modeling (**Eq. 2**) showed significant differences of
 97 the particle source strength $\log_{10} P_M$ for the different vocal loudness conditions piano, mezzoforte
 98 and forte. Vocal loudness affected $\log_{10} P_M$ ($\chi^2(2)=12.47$, $p=0.00196$) lowering it by a factor of
 99 -0.45994 ± 0.11196 (standard errors) from forte to mezzoforte and by a factor of -1.25514 ± 0.23734
 100 (standard errors) from forte to piano. The described higher emission rates for females than for
 101 males failed to reach statistical significance.

102 For all subjects, the intended increase in loudness from piano to forte was reflected in the
 103 measured values of the sound pressure level. Additionally, **Figure 4** shows the relationship between
 104 the emission rate and the maximum sound pressure level (only the median values for experiment II
 105 – sustained vowel /a/ – were considered). An increase in the sound pressure level was accompanied
 106 by a mean increase in the emission rate $\log_{10} P_M$ by a factor of 0.06. With regard to sustained
 107 vowels, it could be stated that the emission rates can vary by more than two orders of magnitude.

108 Discussion

109 Due to the increased risk of transmission of SARS-CoV-2 viruses during singing and the described
 110 accumulation of these infections during choir rehearsals, the survey of particle emissions and the
 111 assessment of aerosols in rooms are key elements in the risk management of ensemble and choir
 112 singing in enclosed rooms.

113 The measuring method used (laser particle counter) provides very high accuracy concerning the
 114 absolute number of particles and their size because sources of interference have been reduced to

Table 1. Ratios of medians of particle source strengths for different test and loudness conditions

ID	Speaking/breathing	Singing/breathing	Singing/speaking	Forte/piano	Forte/mezzoforte
S1	82.99	329.61	3.97	60.81	6.61
S2	0.14	14.22	99.54	19.86	1.46
S3	4.34	124.74	28.77	114.29	2.50
S4	10.50	62.37	5.94	41.98	6.00
S5	6.12	65.31	10.67	0.84	1.46
S6	0.25	15.24	60.95	3.40	1.55
S7	3.78	86.50	22.91	40.36	1.59
S8	19.05	228.03	11.97	44.46	6.35

115 a minimum. Furthermore, the suitability of the peripheral test setup could be proven within the
 116 scope of baseline measurements.

117 An alternative or supplemental method to investigate the size distribution of droplets during
 118 breathing, speaking and singing is the imaging technique of Particle Image Velocimetry (PIV). This
 119 is based on high-resolution photos of the particles, which are illuminated with a laser light, for
 120 example. Studies using PIV also show that more particles are emitted when speaking loudly than
 121 speaking with low voice (*Anfinrud et al., 2020*). However, mainly qualitative statements can be
 122 made here, due to several influencing factors. Size and number of particles can only be estimated,
 123 because of the background concentration of particles in the room and some drops can only be
 124 picked up in a blurred way. In a study of *Chen-Yu et al. (2000)*, particles of the sizes 1, 10, and 100 μm
 125 were measured with PIV and high accuracy was shown for particles greater than 6 μm . This may be
 126 a reason why investigations of the size distribution of droplets with PIV lead to significantly higher
 127 mean particle diameters (*Chao et al., 2009*). Recent studies show that with PIV, particles in the
 128 order of 1 μm can be examined (*Kähler and Hain, 2020*). For particles, in the order of 0.3 – 20 μm ,
 129 the laser particle counter used in cleanroom conditions offers higher accuracy in determining the
 130 number and size of particles.

131 Since the aerosols emitted during breathing, speaking (*Hartmann et al., 2020*) and singing are
 132 mainly < 1 μm in size, it cannot be assumed that they sink quickly to the ground. It had been
 133 shown, that the retention time was in the range of minutes to hours and the sink rate is in the

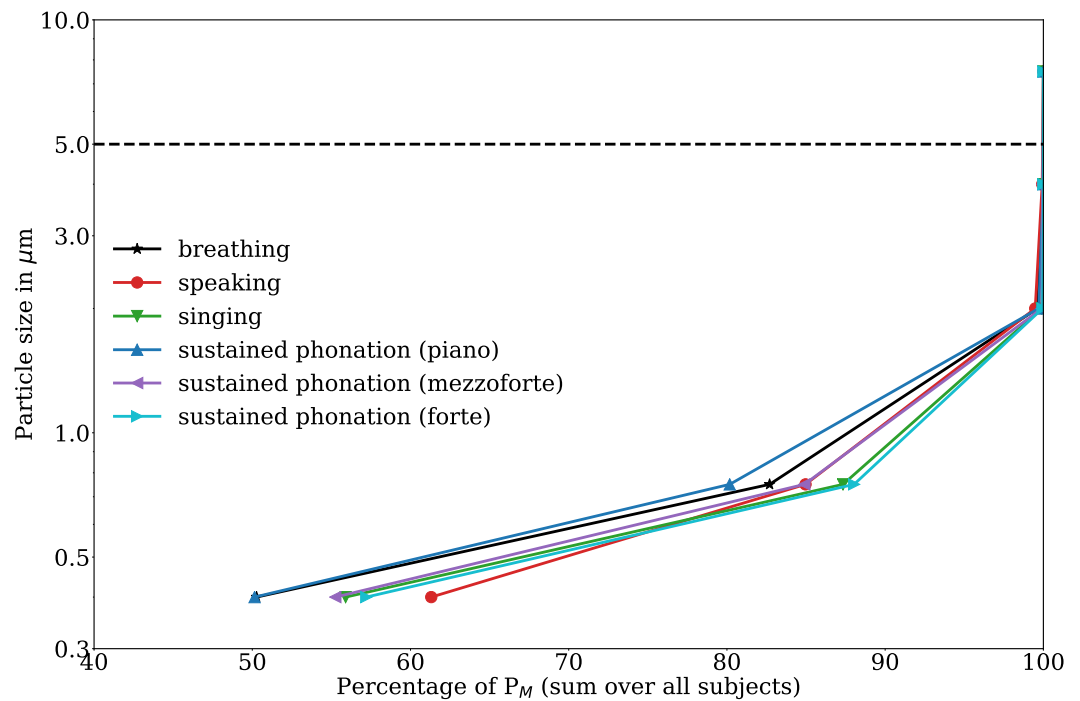


Figure 1. Log-probability plot of the frequency distribution of the size of the detected particles. Regardless of the task, > 99 % of all detected particles are $\leq 5 \mu\text{m}$ (dashed line). Furthermore all tasks show that > 80 % of all particles are $\leq 1 \mu\text{m}$.

134 order of $< 1 \text{ mm/s}$ (*Stadnytskyi et al., 2020; Tellier, 2006*). The determined order of magnitude of
 135 the particle size of this study is significantly lower than the results of the only study, where the
 136 particle emission during singing was also investigated. In this former study, the estimated particle
 137 size during singing was determined with $68 \mu\text{m}$ in median (*Loudon and Roberts, 1967, 1968*).
 138 Furthermore, in the same study, the sizes of the emitted particles for speaking were determined by
 139 $81 \mu\text{m}$. The discrepancy between these and the data presented in this article, is probably due to the
 140 high-precision measuring methods not yet available at that time. With regard to the size of emitted
 141 particles, *Asadi et al. (2019)* was able to show that they are distinctively smaller than $10 \mu\text{m}$ during
 142 speaking and breathing (see also *Papineni and Rosenthal (1997)*).

143 The present study confirms that higher emission rates of aerosols are produced during singing
 144 in comparison to speaking and breathing. *Asadi et al. (2019)* found higher emission rates for
 145 speaking compared to breathing and an increase of emission rates with raising vocal loudness. He
 146 could further show that the range of emission rate ranges from 1 to 100 P/s for speaking, which
 147 roughly confirms our data (14.13 to 390.84, see *Appendix 1, Table 3*). Similar rates of 330 P/s
 148 (particle size ranges between 0.8 to $5.5 \mu\text{m}$) were obtained by *Morawska et al. (2009)* for sustained

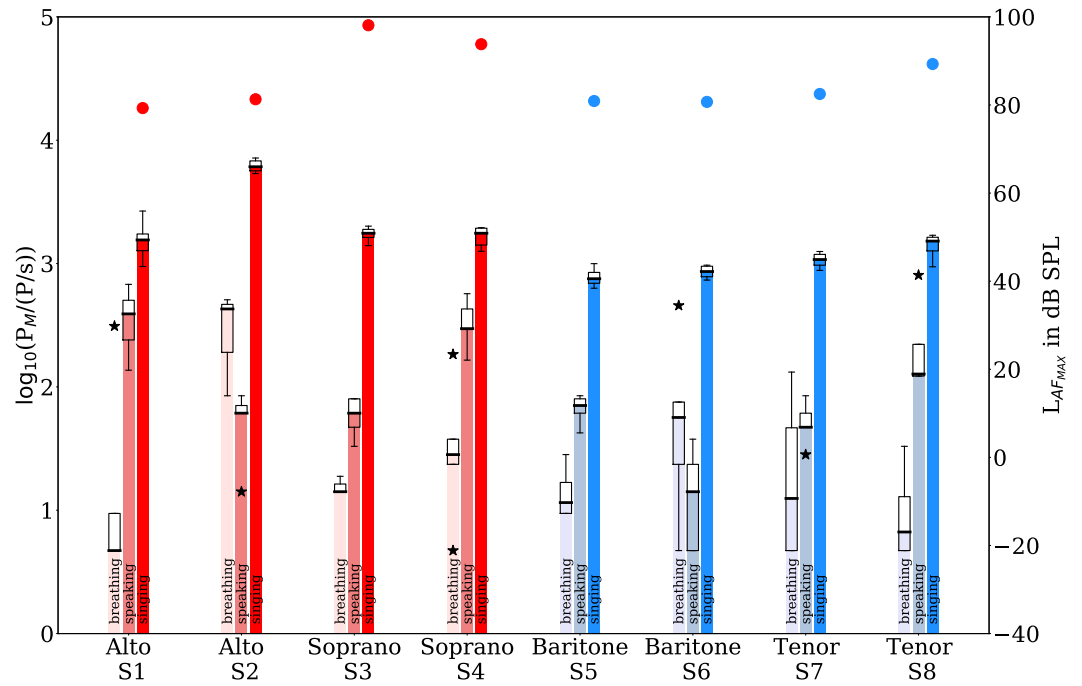


Figure 2. Boxplots of the particle source strengths (bars represent the median) for different gender, voice classifications and the test conditions breathing, speaking and singing in experiment I (left y-axis). Only particles $\leq 5 \mu\text{m}$ were considered. For singing, the maximum sound pressure levels $L_{AF_{MAX}}$ are also shown (full circles, right y-axis).

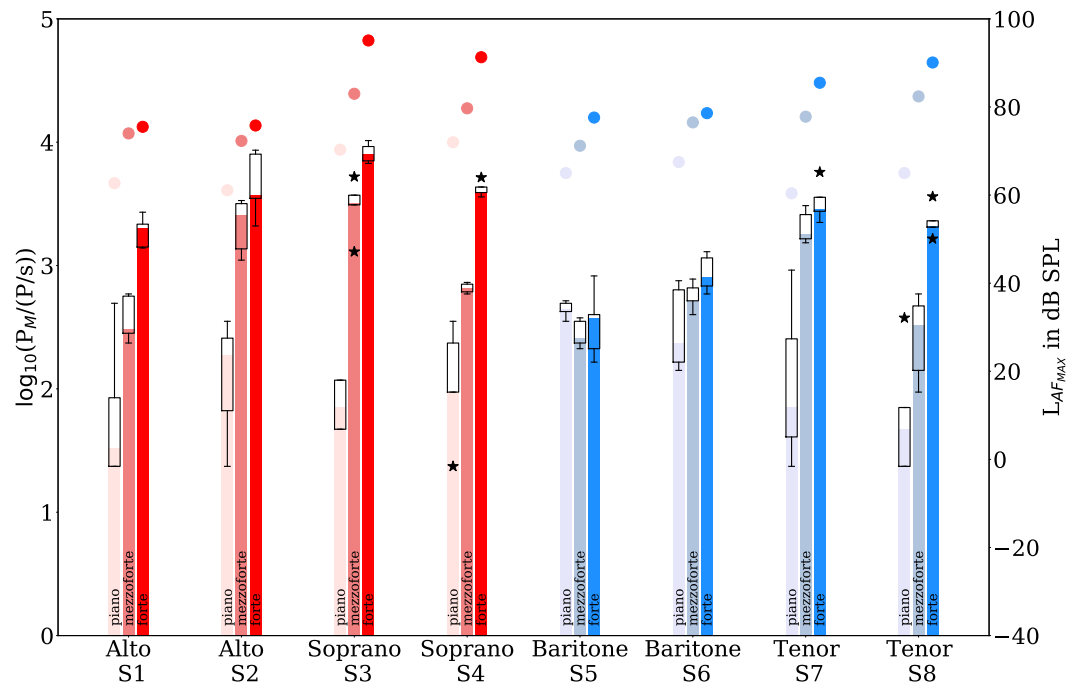


Figure 3. Boxplots of the particle source strengths (bar represents the median) for different gender, voice classifications and vocal loudness conditions while sustaining the vowel /a/ (Experiment II) (left y-axis). Only particles $\leq 5 \mu\text{m}$ were considered. For the different loudness conditions, the maximum sound pressure levels LAF_{MAX} are also shown (full circles, right y-axis).

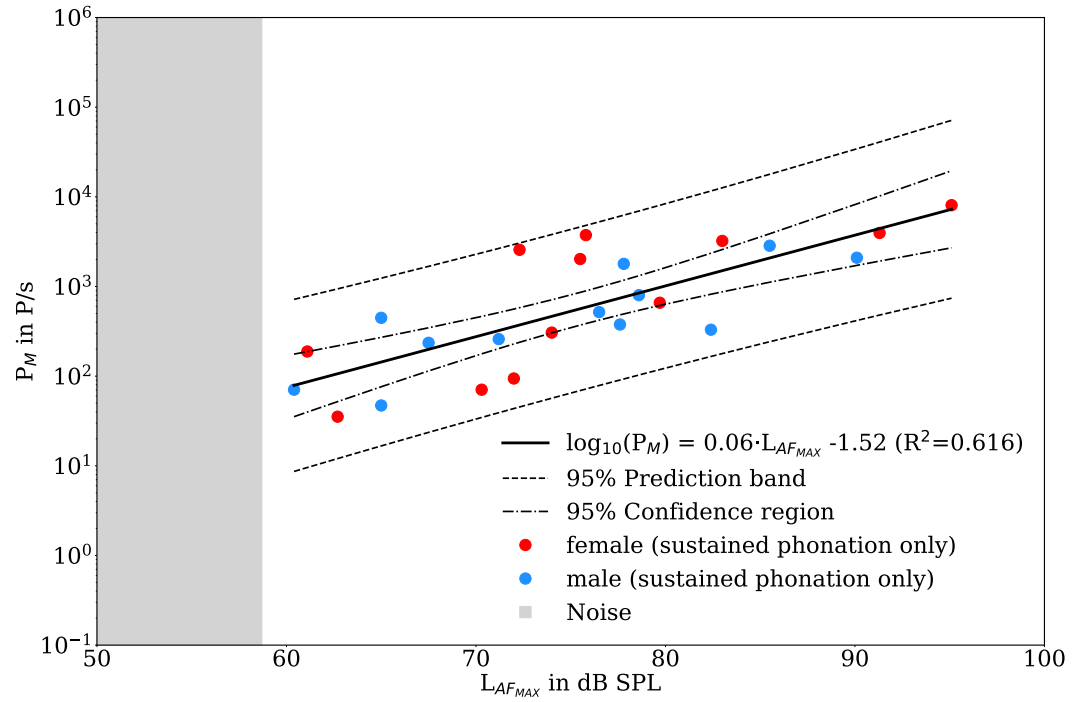


Figure 4. Relationship between particle source strength and the maximum sound pressure level for the test condition of sustained vowel /a/ (Experiment II) for all three loudness conditions separated by gender including linear regression of the logarithmic particle source strengths (black line). Only particles $\leq 5 \mu\text{m}$ were considered. The grey field represents the sound pressure level resulting from the environmental conditions (primarily particle counter) alone.

149 vowels, whereas for unvoiced plosives significantly larger droplets of up to 500 μm were determined
150 (*Anfinrud et al., 2020*). Furthermore, there is a good agreement of the particle source strength in
151 breathing with *Asadi et al. (2019)*.

152 However, phonation of sustained vowels, characterized by a periodic collision of the vocal folds
153 correlating with pitch, does not reflect the ordinary situation in choral singing. Here, the order
154 of consonants and vowels alternate in a sung passage and are interrupted by pauses. Therefore,
155 in the present study, a sequence of 50 seconds of the choir piece "Abschied vom Walde" by Felix
156 Mendelssohn Bartholdy was selected. Each line of the four-part choral movement was sung by
157 the individually appropriate voice classification (soprano, alto, tenor, baritone). These data were
158 compared with the tasks 'breathing' and 'speaking' (reading the standardized text corpus). Again,
159 there is an increase of the emission rate for singing in comparison to speaking. Probably, this is due
160 to the higher ratio of voiced segments to pauses and the increased sound pressure level in singing.
161 Further, these findings agree with the observation that voiced vocalizations lead to higher aerosol
162 emissions (*Asadi et al., 2020a,b*).

163 Apart from the influence of vocal loudness on the emission rate, we found gender differences
164 with higher particle source strengths for female singers. One reason for a stronger aerosol gener-
165 ation might be the higher frequency of the vibrating vocal folds. This counts both, for the higher
166 soprano and alto line of the four-part choral movement and for the selected higher pitch for females
167 during sustained phonation.

168 However, the data presented here show no clear homogeneity within the cohort. For example,
169 the emission rate determined for singing fluctuates by almost one order of magnitude. Also, the
170 increase of P_M between singing and speaking fluctuates by almost two orders of magnitude. Thus,
171 the aspect of high-emitters or super-emitters might be considered (*Asadi et al., 2019*).

172 Of course, the determined emission rate does not provide any information about a possible
173 concentration of SARS-CoV-2 viruses. The probability that a 1 μm sized particle contains a virus has
174 been estimated to only 0.01% (*Stadnytskyi et al., 2020*). However, taking into account an average
175 viral RNA load of $7\text{e-}6$ to $2.35\text{e}9$ per mm^3 (*Wölfel et al., 2020*), it can be estimated that one minute
176 of loud speech produces at least 1000 virus-containing droplet nuclei that can remain in the air
177 up to several hours. However, at present this number can not serve to estimate the probability of
178 infection. (*Bar-On et al., 2020*).

179 It should be noted that in the course of the actual pandemic so far, numerous situations seem

180 to be related to a high probability of aerogenic virus transmission, among them choir rehearsals.
181 There is also initial evidence of viable SARS-CoV-2 viruses in indoor air (*Guo et al., 2020*). However,
182 comprehensive information on the transmission quantity and survivability of SARS-CoV-2 viruses in
183 aerosols is still missing (*van Doremalen et al., 2020*).

184 Therefore, the present study contributes to one component in the risk assessment of singing,
185 which in turn is largely determined by the current prevalence. Finally, there is a lack of data
186 on whether specific breathing characteristics of singing (deep inhalation, higher intrapulmonary
187 pressures) influence the risk of transmission when singing loudly. In any case, the data should
188 support all efforts to improve the risk management, especially in choir singing.

189 **Materials and Methods**

190 **Subjects**

191 Eight singers (ages 22 to 62 years; professional experience between 1 to 34 years) of a professional
192 chamber choir (RIAS Kammerchor Berlin) took part in the investigations. To each of the different
193 voice classifications belonged two of the subject group: alto (S1 & S2), soprano (S3 & S4), baritone
194 (S5 & S6), and tenor (S7 & S8). This study was conducted according to the ethical principles based
195 on the WMA Declaration of Helsinki and to the current legal provisions and informed consent was
196 obtained from all subjects. It should be noted, that the results for breathing and speaking tasks of
197 the subjects considered in this study, have already been analyzed and published within a larger
198 cohort (*Hartmann et al., 2020*). In order to allow a direct comparison with the data for singing, the
199 data of this subgroup were reused and analyzed.

200 **Particle measurements**

201 The investigations were carried out in a cleanroom at the Hermann Rietschel Institute of the
202 Technical University of Berlin.

203 The supply air was introduced via a vertical low-turbulence displacement flow (TAV) over the
204 entire ceiling area of 4.8 x 4.8 m². The supply air velocity was 0.3 m/s and thus prevented thermal
205 lift at the people. The exhaust air was also discharged from the room over the entire surface via a
206 raised floor. The room temperature was 295.15 K ± 0.50 K, the relative humidity was 40 % ± 2 % and
207 the room had 15 Pa overpressure to the surrounding rooms.

208 The actual test stand was located in this highly pure environment (*Figure 5*). It consisted of a

209 glass pipe, in which a constant airflow of 400 m³/h was generated by a filter fan unit (Ziehl-Abegg,
 210 Künzelsau, Deutschland). The measuring probe of a laser particle counter (Lighthouse Solair 3100
 211 E, Lighthouse Worldwide Solutions, Fremont, CA) was placed centrally in the pipe.

212 The particle counter was counting with a volume flow of 28.3 l/min, with a measuring time of
 213 10 seconds each and detected particles in six size classes: > 0.3 μm – 0.5 μm, > 0.5 μm – 1.0 μm,
 214 > 1.0 μm – 3.0, > 3.0 μm – 5.0 μm, > 5.0 μm – 10 μm and > 10 μm.

215 The source strength $\log_{10} P_M$ presented in **Figure 2**, **Figure 3** and **Figure 4** was computed based
 216 on the measured particle concentration c_M and the volume flow through the filter fan unit (FFU)
 217 \dot{V}_{FFU} , i.e.

$$P_M = c_M \cdot \dot{V}_{FFU}. \quad (1)$$

218 To estimate sources of interference, such as background noise of particles in the room, as well as
 219 abrasion on the clothing and hair of the persons investigated, a baseline measurement was carried
 220 out at the beginning of the investigation. For particle reduction due to movement artifacts, the test
 221 persons wore cleanroom clothing and a headgear with the sealing of the edges with adhesive tape,
 222 so that only eyes, nose, and mouth were uncovered.

223 In this baseline measurement, a count rate of the particle counter of <1 particles/5 minutes was
 224 determined within a measurement period of 10 minutes.

225 The counting efficiency for particles of the size 0.3 μm is 50 % ± 20 % and for particles of the size
 226 0.5 μm it is 100 % ± 10 % according to ISO 21501-4. To investigate how many particles were separated
 227 over the measuring distance, comparative measurements were made over a short distance from
 228 the particle counter. For this case, the particles were directly collected through a 150 mm high
 229 funnel while breathing and speaking and directed to the particle counter. The same size distribution
 230 was found as in the finally used configuration.

231 **Audio measurements**

232 The sound pressure level was determined using a calibrated sound level meter (CENTER 322_
 233 Datalogger Sound Level Meter, Center Technologies, Houston, TX). During all measurements, the
 234 sound level meter was located approximately 60 cm anterior-laterally away from the mouth of the
 235 test persons due to limited accessibility. The measuring arrangement of the particle counter did not
 236 allow a standard positioning of 30 cm mouth distance of the measuring device. Furthermore, the

237 high sensitivity of the particle counter did not allow a frontal positioning of the sound level meter
 238 inside the glass tube. Consequently, the determined levels were not to be considered as absolute
 239 levels but are lowered by a constant value of approx. 10 dB SPL.

240 Due to the time variability of the determined sound pressure levels (primarily for speaking and
 241 singing), the maximum value $L_{AF_{MAX}}$ of the frequency- and time-weighted acoustic pressure was
 242 recorded and evaluated.

243 **Test conditions**

244 The subjects were in a sitting position at the entry of the particle measurement setup. Two
 245 experiments were carried out:

246 Experiment I: Comparison of three different test conditions

- 247 a) Breathing through the mouth
- 248 b) Reading a standardized text
- 249 c) Singing a line of a four-part choral movement

250 Experiment II: Singing a sustained vowel (/a/) at three loudness conditions

- 251 a) piano
- 252 b) mezzo-forte
- 253 c) forte

254 For experiment I, respectively, a time window of 50 seconds was analyzed. Further, for experi-
 255 ment II the time window was set to 10 seconds. For reading in a comfortable loudness condition
 256 (1b), the text "Der Nordwind und die Sonne" by Äsop was selected. To pass 1c) the choral part of
 257 the song "Abschied vom Walde" by Felix Mendelssohn-Bartholdy was chosen. The subjects were
 258 instructed to sing the line of their individual voice classification. Each of all tasks were repeated
 259 five times.

260 The following pitches were selected for experiment II: soprano: C5 (523 Hz), alto: F4 (349 Hz),
 261 tenor: C4 (262 Hz), and baritone: F3 (175 Hz). The total measuring time for all tasks was about
 262 30 minutes for each subject.

263 **Statistical Analysis**

264 Besides the description of the data, a confirmative analysis was carried out. Therefore, a linear
 265 mixed effects analysis of the relationship between $\log_{10} P_M$, gender, condition and subject was

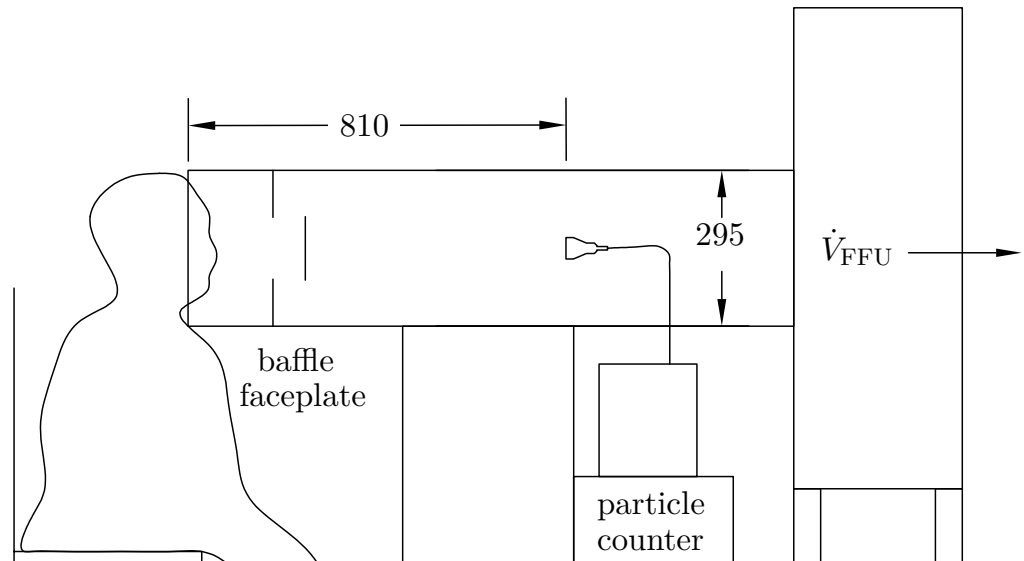


Figure 5. Left: Schematic test setup with one person in cleanroom clothing whose exhaled air was recorded by the particle counter. The glass measuring section was located on the suction side of a horizontally positioned Filter Fan Unit (FFU). All geometric dimensions are in mm (Figure adapted from Fig 2 in *Hartmann et al. (2020)*).

266 performed by means of the freely available software package R (*R Core Team, 2020*) including the
 267 package lme4 (*Bates et al., 2015*) (see *Winter (2013)*). The model used was

$$\log_{10} P_M \sim \text{Condition} + \text{Gender} + (1 + \text{Condition}|\text{Subject}) + (1 + \text{Gender}|\text{Subject}) \quad (2)$$

268 (R model syntax). Condition and gender were incorporated as fixed effects into the model. Intercepts
 269 for subject were incorporated as random effects. To keep the model maximal as proposed by *Barr*
 270 *et al. (2013)*, by--subject random slopes for the effect of gender and condition were additionally
 271 incorporated as random effects. The interaction term between condition and gender was identified
 272 as not significant and therefore not regarded. Careful visual inspection of residual-plots and Q-Q-
 273 plots did reveal obvious deviations from homoscedasticity and normality. Therefore, log-transform
 274 of P_M was considered which overcomes these problems. To avoid infinite values in the analyses, only
 275 $P_M > 0$ were taken into account. To test significance, the P-values were obtained by likelihood ratio
 276 tests of the full model with the effect in question against the model without the effect in question.
 277 For this reason, linear mixed models were fit by maximum likelihood to enable comparison.

278 Acknowledgements

279 We thank the members of the RIAS Kammerchor Berlin for their support.

280 Contributions

281 D. M., M. F., and M. K. designed research. J. L., H. R. and M. F. made measurements. M. F., J. L., D. M.
282 and M. K. wrote the paper.

283 Competing interests

284 The authors declare no competing interest.

285 References

- 286 **Anfinrud P**, Stadnytskyi V, Bax CE, Bax A. Visualizing Speech-Generated Oral Fluid Droplets with Laser Light
287 Scattering. *New England Journal of Medicine*. 2020; <https://www.nejm.org/doi/full/10.1056/NEJMc2007800>,
288 doi: 10.1056/NEJMc2007800.
- 289 **Asadi S**, Bouvier N, Wexler AS, Ristenpart WD. The coronavirus pandemic and aerosols: Does COVID-19 transmit
290 via expiratory particles? *Aerosol Science and Technology*. 2020; 54(6):635–638. [https://doi.org/10.1080/](https://doi.org/10.1080/02786826.2020.1749229)
291 [02786826.2020.1749229](https://doi.org/10.1080/02786826.2020.1749229), doi: 10.1080/02786826.2020.1749229.
- 292 **Asadi S**, Wexler AS, Cappa CD, Barreda S, Bouvier NM, Ristenpart WD. Aerosol emission and superemission
293 during human speech increase with voice loudness. *Scientific Reports*. 2019; 9(1):2348–. [https://doi.org/10.](https://doi.org/10.1038/s41598-019-38808-z)
294 [1038/s41598-019-38808-z](https://doi.org/10.1038/s41598-019-38808-z).
- 295 **Asadi S**, Wexler AS, Cappa CD, Barreda S, Bouvier NM, Ristenpart WD. Effect of voicing and articulation manner
296 on aerosol particle emission during human speech. *PLOS ONE*. 2020 01; 15(1):1–15. [https://doi.org/10.1371/](https://doi.org/10.1371/journal.pone.0227699)
297 [journal.pone.0227699](https://doi.org/10.1371/journal.pone.0227699), doi: 10.1371/journal.pone.0227699.
- 298 **Bar-On YM**, Flamholz A, Phillips R, Milo R. Science Forum: SARS-CoV-2 (COVID-19) by the numbers. *Elife*. 2020;
299 9:e57309. doi: 10.7554/eLife.57309.
- 300 **Barr DJ**, Levy R, Scheepers C, Tily HJ. Random effects structure in mixed-effects models: Keep it maximal. *Journal*
301 *of Memory and Language*. 2013; 68(3):255–278.
- 302 **Bates D**, Mächler M, Bolker B, Walker S. Fitting Linear Mixed-Effects Models Using lme4. *Journal of Statistical*
303 *Software*. 2015; 67(1):1–48. doi: 10.18637/jss.v067.i01.
- 304 **Chao CYH**, Wan MP, Morawska L, Johnson GR, Ristovski ZD, Hargreaves M, Mengersen K, Corbett S, Li Y, Xie X,
305 Katoshevski D. Characterization of expiration air jets and droplet size distributions immediately at the mouth
306 opening. *Journal of Aerosol Science*. 2009; 40(2):122 – 133. [http://www.sciencedirect.com/science/article/pii/](http://www.sciencedirect.com/science/article/pii/S0021850208001882)
307 [S0021850208001882](http://www.sciencedirect.com/science/article/pii/S0021850208001882), doi: <https://doi.org/10.1016/j.jaerosci.2008.10.003>.
- 308 **Chen-Yu C**, Atkinson Joseph F, VanBenschoten John E, Bursik Marcus I, DePinto Joseph V. Image-Based System
309 for Particle Counting and Sizing. *Journal of Environmental Engineering*. 2000 Mar; 126(3):258–266. [https://](https://doi.org/10.1061/(ASCE)0733-9372(2000)126:3(258))
310 [doi.org/10.1061/\(ASCE\)0733-9372\(2000\)126:3\(258\)](https://doi.org/10.1061/(ASCE)0733-9372(2000)126:3(258)), doi: 10.1061/(asce)0733-9372(2000)126:3(258).

- 311 **Couch RB**, Cate TR, Douglas RG, Gerone PJ, Knight V. Effect of route of inoculation on experimental respiratory
312 viral disease in volunteers and evidence for airborne transmission. *Microbiology and Molecular Biology*
313 *Reviews*. 1966; 30(3):517–529. <https://mibr.asm.org/content/30/3/517>.
- 314 **van Doremalen N**, Bushmaker T, Morris DH, Holbrook MG, Gamble A, Williamson BN, Tamin A, Harcourt
315 JL, Thornburg NJ, Gerber SI, Lloyd-Smith JO, de Wit E, Munster VJ. Aerosol and Surface Stability of SARS-
316 CoV-2 as Compared with SARS-CoV-1. *New England Journal of Medicine*. 2020; 382(16):1564–1567. <https://doi.org/10.1056/NEJMc2004973>, doi: 10.1056/NEJMc2004973.
- 317
- 318 **Guo ZD**, Wang ZY, Zhang SF, Li X, Li L, Li C, Cui Y, Fu RB, Dong YZ, Chi XY, Zhang MY, Liu K, Cao C, Liu B,
319 Zhang K, Gao YW, Lu B, Chen W. Aerosol and Surface Distribution of Severe Acute Respiratory Syndrome
320 Coronavirus 2 in Hospital Wards, Wuhan, China, 2020. *Emerging Infectious Disease journal*. 2020; 26(7):1583.
321 https://wwwnc.cdc.gov/eid/article/26/7/20-0885_article.
- 322 **Hamner L**, Dubbel P, Capron I, Ross A, Jordan A, Lee J, Lynn J, Ball A, Narwal S, Russell S, Patrick D, H L. High
323 SARS-CoV-2 Attack Rate Following Exposure at a Choir Practice – Skagit County, Washington, March 2020.
324 *MMWR Morb Mortal Wkly Rep*. 2020; 69:606–610. doi: 10.15585/mmwr.mm6919e6.
- 325 **Hartmann A**, Lange J, Rotheudt H, Kriegel M. Emission rate and particle size of bioaerosols during breathing,
326 speaking and coughing; 2020, <http://dx.doi.org/10.14279/depositonce-10331>, doi: 10.14279/depositonce-
327 10331, preprint Technische Universität Berlin.
- 328 **Johnson G**, Morawska L, Ristovski Z, Hargreaves M, Mengersen K, Chao CYH, Wan M, Li Y, Xie X, Katoshevski D,
329 et al. Modality of human expired aerosol size distributions. *Journal of Aerosol Science*. 2011; 42(12):839–851.
330 doi: 10.1016/j.jaerosci.2011.07.009.
- 331 **Johnson GR**, Morawska L. The mechanism of breath aerosol formation. *Journal of Aerosol Medicine and*
332 *Pulmonary Drug Delivery*. 2009; 22(3):229–237. doi: 10.1089/jamp.2008.0720.
- 333 **Judson SD**, Munster VJ. Nosocomial Transmission of Emerging Viruses via Aerosol-Generating Medical Proce-
334 dures. *Viruses*. 2019 Oct; 11(10):940. <https://pubmed.ncbi.nlm.nih.gov/31614743>.
- 335 **Kähler CJ**, Hain R. Fundamental protective mechanisms of face masks against droplet infections. *Journal of*
336 *Aerosol Science*. 2020; 148:105617. <http://www.sciencedirect.com/science/article/pii/S0021850220301063>,
337 doi: <https://doi.org/10.1016/j.jaerosci.2020.105617>.
- 338 **Loudon RG**, Roberts RM. Relation between the Airborne Diameters of Respiratory Droplets and the Diameter
339 of the Stains left after Recovery. *Nature*. 1967 Jan; 213(5071):95–96. <https://doi.org/10.1038/213095a0>.
- 340 **Loudon RG**, Roberts RM. Singing and the Dissemination of Tuberculosis. *American Review of Respira-*
341 *tory Disease*. 1968; 98(2):297–300. <https://www.atsjournals.org/doi/abs/10.1164/arrd.1968.98.2.297>, doi:
342 [10.1164/arrd.1968.98.2.297](https://doi.org/10.1164/arrd.1968.98.2.297), PMID: 5667756.

- 343 **Morawska L.** Droplet fate in indoor environments, or can we prevent the spread of infection? *Indoor*
344 *Air.* 2006; 16(5):335–347. <https://onlinelibrary.wiley.com/doi/abs/10.1111/j.1600-0668.2006.00432.x>, doi:
345 [10.1111/j.1600-0668.2006.00432.x](https://doi.org/10.1111/j.1600-0668.2006.00432.x).
- 346 **Morawska L**, Johnson GR, Ristovski ZD, Hargreaves M, Mengersen K, Corbett S, Chao CYH, Li Y, Katoshevski D.
347 Size distribution and sites of origin of droplets expelled from the human respiratory tract during expiratory
348 activities. *Journal of Aerosol Science.* 2009; 40(3):256 – 269. [http://www.sciencedirect.com/science/article/pii/](http://www.sciencedirect.com/science/article/pii/S0021850208002036)
349 [S0021850208002036](http://www.sciencedirect.com/science/article/pii/S0021850208002036), doi: <https://doi.org/10.1016/j.jaerosci.2008.11.002>.
- 350 **Morawska L**, Cao J. Airborne transmission of SARS-CoV-2: The world should face the reality. *Environment*
351 *International.* 2020; p. 105730. doi: [10.1016/j.envint.2020.105730](https://doi.org/10.1016/j.envint.2020.105730).
- 352 **Papineni RS**, Rosenthal FS. The Size Distribution of Droplets in the Exhaled Breath of Healthy Human Sub-
353 jects. *Journal of Aerosol Medicine.* 1997; 10(2):105–116. <https://doi.org/10.1089/jam.1997.10.105>, doi:
354 [10.1089/jam.1997.10.105](https://doi.org/10.1089/jam.1997.10.105), PMID: 10168531.
- 355 **R Core Team.** R: A Language and Environment for Statistical Computing. R Foundation for Statistical Computing,
356 Vienna, Austria; 2020, <https://www.R-project.org/>.
- 357 **Stadnytskyi V**, Bax CE, Bax A, Anfinrud P. The airborne lifetime of small speech droplets and their potential im-
358 portance in SARS-CoV-2 transmission. *Proceedings of the National Academy of Sciences.* 2020; 117(22):11875–
359 11877. <https://www.pnas.org/content/117/22/11875>, doi: [10.1073/pnas.2006874117](https://doi.org/10.1073/pnas.2006874117).
- 360 **Tellier R.** Review of aerosol transmission of influenza A virus. *Emerging infectious diseases.* 2006 Nov;
361 12(11):1657–1662. <https://pubmed.ncbi.nlm.nih.gov/17283614>.
- 362 **Wei J**, Li Y. Enhanced spread of expiratory droplets by turbulence in a cough jet. *Building and Envi-*
363 *ronment.* 2015; 93:86 – 96. <http://www.sciencedirect.com/science/article/pii/S0360132315300329>, doi:
364 <https://doi.org/10.1016/j.buildenv.2015.06.018>.
- 365 **Winter B**, *Linear models and linear mixed effects models in R with linguistic applications*; 2013.
- 366 **Wölfel R**, Corman VM, Guggemos W, Seilmaier M, Zange S, Müller MA, Niemeyer D, Jones TC, Vollmar P,
367 Rothe C, Hoelscher M, Bleicker T, Brünink S, Schneider J, Ehmann R, Zwirgmaier K, Drosten C, Wendtner
368 C. Virological assessment of hospitalized patients with COVID-2019. *Nature.* 2020 May; 581(7809):465–469.
369 <https://doi.org/10.1038/s41586-020-2196-x>.

370 **Appendix 1****Appendix 1 Table 1.** Minimum, maximum, median values and interquartile ranges of particle source strengths for singing

ID	Min	Max	Median	Interquartile range
S1	946.24	2666.86	1552.39	1.37
S2	5370.32	7177.94	6095.37	1.21
S3	1399.59	2009.09	1761.98	1.16
S4	1256.03	1954.34	1761.98	1.37
S5	630.96	997.70	753.36	1.22
S6	734.51	970.51	860.99	1.22
S7	881.05	1253.14	1078.95	1.22
S8	941.89	1694.34	1520.55	1.29

Appendix 1 Table 2. Minimum, maximum, median values and interquartile ranges of particle source strengths for speaking

ID	Min	Max	Median	Interquartile range
S1	136.46	677.64	390.84	2.10
S2	14.13	84.72	61.24	1.15
S3	32.96	79.98	61.24	1.70
S4	164.82	570.16	296.48	1.47
S5	42.36	84.72	70.63	1.31
S6	4.71	37.67	14.13	5.00
S7	28.25	84.72	47.10	1.30
S8	122.46	805.38	127.06	1.81

Appendix 1 Table 3. Minimum, maximum, median values and interquartile ranges of particle source strengths for breathing

ID	Min	Max	Median	Interquartile range
S1	4.71	310.46	4.71	2.00
S2	84.72	508.16	428.55	2.45
S3	14.13	18.84	14.13	1.15
S4	4.71	183.65	28.25	1.60
S5	9.42	28.25	11.53	1.78
S6	4.71	457.09	56.49	3.20
S7	4.71	131.83	12.47	9.89
S8	4.71	32.96	6.67	2.74

Appendix 1 Table 4. Minimum, maximum, median values and interquartile ranges of particle source strengths for piano

ID	Min	Max	Median	Interquartile range
S1	23.55	494.31	33.27	3.60
S2	23.55	353.18	188.36	3.87
S3	47.10	117.76	70.63	2.50
S4	23.55	353.18	94.19	2.50
S5	353.18	517.61	447.71	1.17
S6	141.25	753.36	235.50	3.85
S7	23.55	918.33	70.63	6.25
S8	23.55	376.70	47.10	3.00

Appendix 1 Table 5. Minimum, maximum, median values and interquartile ranges of particle source strengths for forte

ID	Min	Max	Median	Interquartile range
S1	1389.95	2710.19	2023.02	1.53
S2	2094.11	8609.94	3741.11	2.28
S3	6729.77	10303.86	8072.35	1.31
S4	3605.79	5176.07	3953.67	1.11
S5	164.82	824.14	376.70	1.89
S6	588.84	1294.20	799.83	1.69
S7	2238.72	5714.79	2851.02	1.30
S8	1648.16	3622.43	2094.11	1.13

Appendix 1 Table 6. Minimum, maximum, median values and interquartile ranges of particle source strengths for mezzoforte

ID	Min	Max	Median	Interquartile range
S1	235.50	588.84	306.20	2.00
S2	1106.62	3365.12	2564.48	2.33
S3	1294.20	5248.07	3228.49	1.20
S4	588.84	729.46	659.17	1.15
S5	211.84	376.70	258.82	1.50
S6	399.94	776.25	517.61	1.27
S7	1531.09	3061.96	1790.61	1.57
S8	94.19	588.84	329.61	3.33